

Study of CP violation in B^\pm decays to $\overline{D^0}(D^0)K^\pm$ at FCCee

R. Aleksan¹, L. Oliver² and E. Perez³

¹ IRFU, CEA, Université Paris-Saclay, 91191 Gif-sur-Yvette cedex, France

² IJCLab, Pôle Théorie, CNRS/IN2P3 et Université Paris-Saclay, bât. 210, 91405 Orsay, France

³ CERN, EP Department, Geneva, Switzerland

October 12, 2022

ABSTRACT

The great progress made recently in the sector of Flavor Physics has enabled to establish CP violation in the B-meson decays. The unitarity triangle derived from the unitarity relation $V_{ub}^*V_{ud} + V_{cb}^*V_{cd} + V_{tb}^*V_{td} = 0$ has been measured very precisely. To further assess our understanding of CP violation, it would be useful to carry out similar measurement of other triangles. In this note, we investigate the triangle derived from the relation $V_{ub}^*V_{us} + V_{cb}^*V_{cs} + V_{tb}^*V_{ts} = 0$. Two angles of this triangle (α_s and β_s) could be measured very accurately at FCCee using the decays $B_s(\overline{B}_s) \rightarrow D_s^\pm K^\mp$ and $B_s(\overline{B}_s) \rightarrow J/\psi\phi$ respectively, as discussed elsewhere by us. This note concentrates on the measurement of the third angle γ_s using the modes $B^\pm \rightarrow \overline{D^0}(D^0)K^\pm$. We show that a direct measurement of the angle γ_s is possible with some specific B^\pm decays with an estimated resolution of the order of 1° .

1 Introduction

The purpose of this note is to discuss the general features of the reactions $B^+ \rightarrow \overline{D^0}(D^0)K^+$, in particular with respect to the interference effects which one expects in the Standard Model (SM).

Should there be only 3 families, the CKM matrix elements obey the following triangular unitarity relations,

$$\begin{aligned} UT_{bd} &\equiv V_{ub}^*V_{ud} + V_{cb}^*V_{cd} + V_{tb}^*V_{td} = 0 \\ UT_{sb} &\equiv V_{ub}^*V_{us} + V_{cb}^*V_{cs} + V_{tb}^*V_{ts} = 0 \\ UT_{ds} &\equiv V_{us}^*V_{ud} + V_{cs}^*V_{cd} + V_{ts}^*V_{td} = 0 \end{aligned} \tag{1}$$

In the first equation (1), UT_{bd} is known as the Unitarity Triangle, with the three sides of the same order. The second equation corresponds to a significantly flatter triangle, while the third one is almost completely flat. These triangles are visualized in Fig. 1.

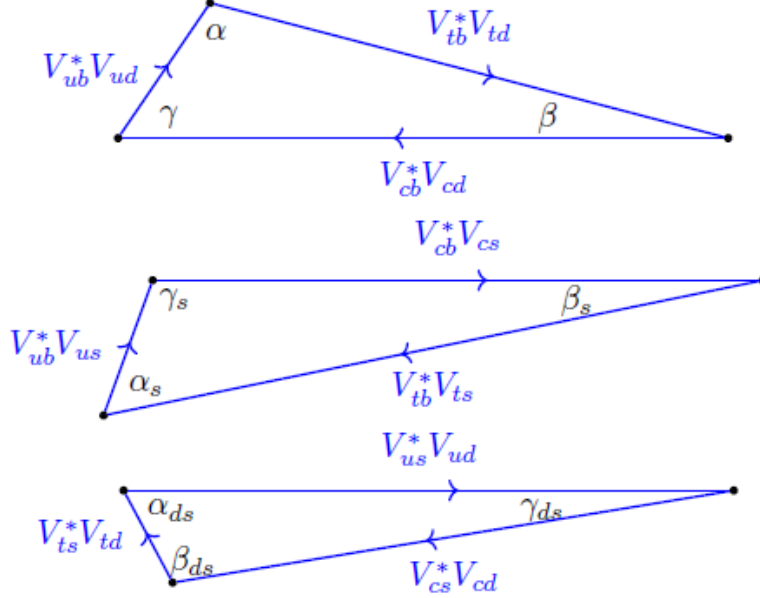


Fig. 1. Unitarity Triangle UT_{bd} involving the 3rd and 1st columns (top), Unitarity Triangle UT_{sb} involving the 2nd and 3rd columns (center) and Unitarity Triangle UT_{ds} involving the 1nd and 2nd columns (bottom) of the CKM matrix (not to scale).

There are also three additional triangles, but they are very similar to those above. In the SM, the CKM matrix has only four independent parameters. Therefore the angles of these triangles can be expressed in terms of four angles. The first relation in (1), with the three sides of the same order, has been studied extensively. However the other ones would deserve to be studied in detail as well, in order to investigate further the consistency of the SM.

We define the angles of these triangles as

$$\begin{aligned}
 \alpha &= \arg\left(-\frac{V_{tb}^*V_{td}}{V_{ub}^*V_{ud}}\right), & \beta &= \arg\left(-\frac{V_{cb}^*V_{cd}}{V_{tb}^*V_{td}}\right), & \gamma &= \arg\left(-\frac{V_{ub}^*V_{ud}}{V_{cb}^*V_{cd}}\right) \\
 \alpha_s &= \arg\left(-\frac{V_{ub}^*V_{us}}{V_{tb}^*V_{ts}}\right), & \beta_s &= \arg\left(-\frac{V_{tb}^*V_{ts}}{V_{cb}^*V_{cs}}\right), & \gamma_s &= \arg\left(-\frac{V_{cb}^*V_{cs}}{V_{ub}^*V_{us}}\right) \\
 \alpha_{ds} &= \arg\left(-\frac{V_{us}^*V_{ud}}{V_{ts}^*V_{td}}\right), & \beta_{ds} &= \arg\left(-\frac{V_{ts}^*V_{td}}{V_{cs}^*V_{cd}}\right), & \gamma_{ds} &= \arg\left(-\frac{V_{cs}^*V_{cd}}{V_{us}^*V_{ud}}\right)
 \end{aligned} \tag{2}$$

After having studied the direct determination of the angles α_s and β_s at FCCee in ref. [1], in the present paper we are interested and we focus on the

direct determination of the angle γ_s of the "rather flat" triangle UT_{sb} . By *direct determination* of one angle we mean measurement of the angle without making use of its relations to other angles of the triangles in the SM [2].

2 Study of interference effect for the reactions $B^+ \rightarrow \overline{D^0}(D^0)K^+$ and their CP conjugates.

The decays $B^+ \rightarrow \overline{D^0}K^+$ and $B^+ \rightarrow D^0K^+$, as well as their CP conjugates, can interfere in some specific cases. These decays are penguin-free and their interference may lead to clean measurement of the CKM phase involved and will be discussed in the following.

2.1 Direct CP violation in B^+ decays

We first investigate how CP violation can be generated with the modes $B^+ \rightarrow \overline{D^0}(D^0)K^+$. The decay diagrams for these mode are shown in Fig. 2 and Fig. 3.

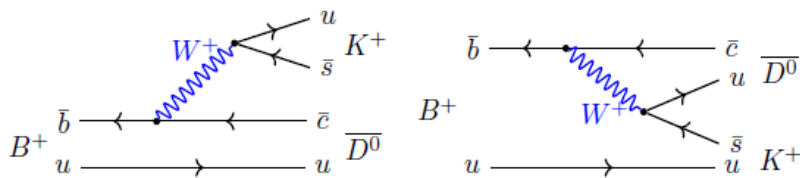


Fig. 2. The leading Feynman diagrams for the B^+ decay for the final state $\overline{D^0}K^+$. The product of CKM elements involved is $V_{cb}^*V_{us}$.

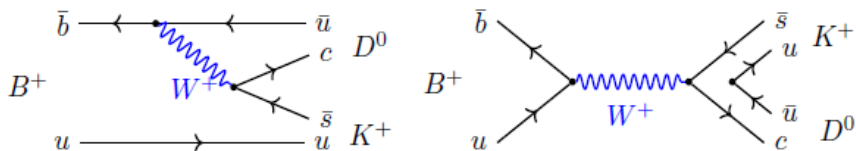


Fig. 3. The leading Feynman diagrams for the B^+ decay for the final state D^0K^+ . The product of CKM elements involved is $V_{ub}^*V_{cs}$.

To generate CP violation in the Standard Model (SM), at least two interfering amplitudes with different strong phases and different weak phases are required. The diagrams in Fig. 2 and in Fig. 3 have distinct CKM weak phases and different strong phases and thus their interference would generate CP violation. This is not always possible since, in general, the final states of $\overline{D^0}$ and D^0 are different, however there are two ways to get around this by selecting specific $\overline{D^0}(D^0)$ decay final states.

1. Using Doubly Cabibbo Suppressed (DCS) final states for $\overline{D^0}$ decays, e.g. $\overline{D^0} \rightarrow K^- \pi^+$, while using the Cabibbo Allowed (CA) final states for D^0 decays, i.e. $D^0 \rightarrow K^- \pi^+$. Obviously, similarly, one may use CA states for $\overline{D^0}$ decays and DCS states for D^0 decays.

2. Using $\overline{D^0}(D^0)$ decays to CP eigenstates, e.g. $\overline{D^0}(D^0) \rightarrow \pi^+\pi^-, K^+K^-$ or $K_s\pi^0$.

One can easily increase the interesting final states by adding π^0 in the final states.

Let us write for illustration two generic interfering amplitudes and their CP conjugates, following the diagrams of Figs. 2 and 3.

$$\begin{aligned}
A_1 &= A(B^+ \rightarrow \overline{D^0}K^+ \rightarrow f_iK^+) = a_1 e^{i\alpha_1} e^{i\Phi_1} \\
A_2 &= A(B^+ \rightarrow D^0K^+ \rightarrow f_iK^+) = a_2 e^{i\alpha_2} e^{i\Phi_2} \\
\overline{A}_1 &= A(B^- \rightarrow D^0K^- \rightarrow \overline{f}_iK^-) = a_1 e^{i\alpha_1} e^{-i\Phi_1} \\
\overline{A}_2 &= A(B^- \rightarrow \overline{D^0}K^- \rightarrow \overline{f}_iK^-) = a_2 e^{i\alpha_2} e^{-i\Phi_2}
\end{aligned} \tag{3}$$

where $a_1(a_2)$ are real numbers, $\alpha_1(\alpha_2)$ are the strong phases and $\Phi_1(\Phi_2)$ are the weak phases. With the notation $\Delta = \alpha_1 - \alpha_2$ and $\Phi = \Phi_1 - \Phi_2$, one can write the partial widths

$$\begin{aligned}
|A|^2 &= |A_1 + A_2|^2 = a_1^2 + a_2^2 + 2a_1a_2[\cos \Delta \cos \Phi - \sin \Delta \sin \Phi] \\
|\overline{A}|^2 &= |\overline{A}_1 + \overline{A}_2|^2 = a_1^2 + a_2^2 + 2a_1a_2[\cos \Delta \cos \Phi + \sin \Delta \sin \Phi]
\end{aligned} \tag{4}$$

Should one know a_1^2 and a_2^2 , one is left with two equations with two unknowns, Δ and Φ . However this is not trivial as discussed below.

Let us rewrite equations (4) for the final state corresponding to diagrams in Fig. 2 and Fig. 3, with D^0 and $\overline{D^0}$ decaying into a common final state f_i .

The amplitudes A_1 and A_2 will respectively correspond e.g. to the decay chains $B^+ \rightarrow \overline{D^0}K^+ \rightarrow f_iK^+$ and $B^+ \rightarrow D^0K^+ \rightarrow f_iK^+$. We will have then, factorizing $\Gamma[B^+ \rightarrow \overline{D^0}K^+ \rightarrow f_iK^+]$ for the decay $\Gamma(B^+ \rightarrow (f_i)_DK^+)$, and proceeding likewise for its CP conjugate :

$$\begin{aligned}
|A|^2 &\equiv \Gamma(B^+ \rightarrow (f_i)_DK^+) = \Gamma[B^+ \rightarrow \overline{D^0}K^+ \rightarrow f_iK^+] \\
&\quad \times [1 + \mathcal{R}_{B \rightarrow f_iK}^2 + 2\mathcal{R}_{B \rightarrow f_iK}(\cos \Delta_{f_i} \cos \Phi_{f_i} - \sin \Delta_{f_i} \sin \Phi_{f_i})] \\
|\overline{A}|^2 &\equiv \Gamma(B^- \rightarrow (\overline{f}_i)_DK^-) = \Gamma[B^- \rightarrow D^0K^- \rightarrow \overline{f}_iK^-] \\
&\quad \times [1 + \overline{\mathcal{R}}_{B \rightarrow \overline{f}_i\overline{K}}^2 + 2\overline{\mathcal{R}}_{B \rightarrow \overline{f}_i\overline{K}}(\cos \Delta_{\overline{f}_i} \cos \Phi_{\overline{f}_i} - \sin \Delta_{\overline{f}_i} \sin \Phi_{\overline{f}_i})]
\end{aligned} \tag{5}$$

where $f_i(\overline{f}_i)$ is a final state *common* to $\overline{D^0}$ and D^0 , the strong and weak phases satisfy

$$\Delta_{f_i} = \Delta_{\overline{f}_i} = \alpha_1 - \alpha_2, \quad \Phi_{f_i} = -\Phi_{\overline{f}_i} = \Phi_1 - \Phi_2 \tag{6}$$

and the ratios in (5) are defined by

$$\mathcal{R}_{B \rightarrow f_iK} = \sqrt{\frac{\Gamma[B^+ \rightarrow D^0K^+ \rightarrow f_iK^+]}{\Gamma[B^+ \rightarrow \overline{D^0}K^+ \rightarrow f_iK^+]}}$$

$$\begin{aligned}
&= \sqrt{\frac{\Gamma[B^+ \rightarrow D^0 K^+]}{\Gamma[B^+ \rightarrow \overline{D^0} K^+]}} \times \sqrt{\frac{\Gamma[D^0 \rightarrow f_i]}{\Gamma[\overline{D^0} \rightarrow f_i]}} \equiv \mathcal{R} \times \mathcal{R}_{D \rightarrow f_i} \\
&\quad \overline{\mathcal{R}}_{B \rightarrow \overline{f_i} K} = \sqrt{\frac{\Gamma[B^- \rightarrow \overline{D^0} K^- \rightarrow \overline{f_i} K^-]}{\Gamma[B^- \rightarrow D^0 K^- \rightarrow \overline{f_i} K^-]}} \\
&= \sqrt{\frac{\Gamma[B^- \rightarrow \overline{D^0} K^-]}{\Gamma[B^- \rightarrow D^0 K^-]}} \times \sqrt{\frac{\Gamma[\overline{D^0} \rightarrow f_i]}{\Gamma[D^0 \rightarrow f_i]}} \equiv \overline{\mathcal{R}} \times \overline{\mathcal{R}}_{D \rightarrow \overline{f_i}} \quad (7)
\end{aligned}$$

One has the relations

$$\mathcal{R} = \overline{\mathcal{R}}, \quad \mathcal{R}_{D \rightarrow f_i} = \overline{\mathcal{R}}_{D \rightarrow \overline{f_i}} = \frac{1}{\mathcal{R}_{D \rightarrow \overline{f_i}}} \quad (8)$$

that imply

$$\mathcal{R}_{B \rightarrow f_i K} = \overline{\mathcal{R}}_{B \rightarrow \overline{f_i} K} \quad (9)$$

and from eqns. (5)-(9) one gets finally, after some algebra,

$$\begin{aligned}
&\Gamma(B^- \rightarrow (\overline{f_i})_D K^-) = \Gamma[B^+ \rightarrow \overline{D^0} K^+ \rightarrow f_i K^+] \\
&\quad \times [1 + \mathcal{R}_{B \rightarrow f_i K}^2 + 2\mathcal{R}_{B \rightarrow f_i K}(\cos \Delta_{f_i} \cos \Phi_{f_i} + \sin \Delta_{f_i} \sin \Phi_{f_i})] \quad (10)
\end{aligned}$$

From an experimental point of view, $|A|^2$ ($|\overline{A}|^2$) is the number of events $B^+ \rightarrow (f_i)_D K^+$ ($B^- \rightarrow (\overline{f_i})_D K^-$) (i.e. the measured signal), while $\Gamma[B^+ \rightarrow \overline{D^0} K^+ \rightarrow f_i K^+]$ is the number of $B^+ \rightarrow \overline{D^0} K^+$ followed by $\overline{D^0} \rightarrow f_i$ decays.

Looking at the first eqn. (5) and eqn. (10), we have 4 unknowns, $\Gamma[B^+ \rightarrow \overline{D^0} K^+ \rightarrow f_i K^+]$, $\mathcal{R}_{B \rightarrow f_i K}$, Δ_{f_i} and Φ_{f_i} .

With presently operating and future accelerators like LHC, superKEKB and FCC, it should be possible to measure \mathcal{R} and $\mathcal{R}_{D \rightarrow f_i}$, and thus $\mathcal{R}_{B \rightarrow f_i K}$, with high accuracy for most of the relevant final states.

Indeed, one has,

$$\begin{aligned}
\mathcal{R}^2 &= \frac{Br(B^+ \rightarrow D^0 K^+)}{Br(B^+ \rightarrow \overline{D^0} K^+)} = \frac{Br(B^- \rightarrow \overline{D^0} K^-)}{Br(B^- \rightarrow D^0 K^-)} \\
\mathcal{R}_{D \rightarrow f_i}^2 &= \frac{Br(D^0 \rightarrow f_i)}{Br(\overline{D^0} \rightarrow f_i)} = \frac{Br(\overline{D^0} \rightarrow \overline{f_i})}{Br(D^0 \rightarrow \overline{f_i})} \quad (11)
\end{aligned}$$

and these fractions can be determined experimentally, as we argue below

- \mathcal{R} is measured by using semileptonic decays of the $\overline{D^0}(D^0)$. Indeed, the decays $D^0 \rightarrow \ell^+ \nu K^-$ and $\overline{D^0} \rightarrow \ell^- \bar{\nu} K^+$, the Branching Fractions of which are known precisely, tag the flavor of the D mesons.

- As for the decays $\overline{D^0}(D^0) \rightarrow f_i$, they can be determined from the $D^{*+} \rightarrow D^0 \pi^+$ and $D^{*-} \rightarrow \overline{D^0} \pi^-$ decays, where the charge of the pion identifies the flavor of the D^0 meson. The $D^0 - \overline{D^0}$ mixing leads to a negligible effect in the extraction of the Branching Fractions, as expected in the SM.

In summary, we are left with two equations and three unknowns. In principle, $\Gamma[B^+ \rightarrow \overline{D^0}K^+ \rightarrow f_i K^+]$ could be also obtained experimentally. The corresponding number of events is

$$N_{B^+ \rightarrow \overline{D^0}K^+ \rightarrow f_i K^+} = N_{B^+} \times Br(B^+ \rightarrow \overline{D^0}K^+) \times Br(\overline{D^0} \rightarrow f_i) \quad (12)$$

Since the individual branching fractions are known, should one know precisely the initial number of B^+ , one would extract the $N_{B^+ \rightarrow \overline{D^0}K^+ \rightarrow f_i K^+}$. At the Z-pole N_{B^+} is known with a precision of $\sim 2\%$. Although this is not too bad and might be improved at FCCee, it is preferable to keep $N_{B^+ \rightarrow \overline{D^0}K^+ \rightarrow f_i K^+}$ as a free parameter, in which case one would need to use an additional final state f_i as is discussed in [3].

One also derives the CP asymmetry :

$$A_{CP} = \frac{|A|^2 - |\overline{A}|^2}{|A|^2 + |\overline{A}|^2} = \frac{-2\mathcal{R}_{B \rightarrow f_i K} \sin \Delta_{f_i} \sin \Phi_{f_i}}{1 + \mathcal{R}_{B \rightarrow f_i K}^2 + 2\mathcal{R}_{B \rightarrow f_i K} \cos \Delta_{f_i} \cos \Phi_{f_i}} \quad (13)$$

Let us now investigate further the three types of decays mentioned above.

2.2 Using Doubly Cabibbo Suppressed $\overline{D^0}$ decays

In the following we consider the decay $B^+ \rightarrow \overline{D^0}K^+ \rightarrow (K^-\pi^+)_{\overline{D^0}}K^+$ and $B^+ \rightarrow D^0K^+ \rightarrow (K^-\pi^+)_{D^0}K^+$, where the former decay channel is Doubly Cabibbo Suppressed for the decay $\overline{D^0} \rightarrow K^-\pi^+$ and the latter Cabibbo Allowed for $D^0 \rightarrow K^-\pi^+$. Using this type of decays is known as the ADS method [3]. The complete amplitudes read :

$$\begin{aligned} A_{DCS} &= a_{DCS} e^{i\alpha_1} e^{i\Phi_{DCS}} , & A_{CA} &= a_{CA} e^{i\alpha_2} e^{i\Phi_{CA}} \\ \overline{A}_{DCS} &= a_{DCS} e^{i\alpha_1} e^{-i\Phi_{DCS}} , & \overline{A}_{CA} &= a_{CA} e^{i\alpha_2} e^{-i\Phi_{CA}} \end{aligned} \quad (14)$$

where the subscripts DCS and CA stand for Doubly Cabibbo Suppressed and Cabibbo Allowed, respectively.

The CP violating phases in (14) read,

$$\Phi_{DCS} = \arg(V_{cb}^* V_{us} V_{us}^* V_{cd}) , \quad \Phi_{CA} = \arg(V_{ub}^* V_{cs} V_{cs}^* V_{ud}) \quad (15)$$

and one gets

$$\begin{aligned} \Phi_{K^-\pi^+} &= \Phi_{DCS} - \Phi_{CA} = \arg\left(\frac{V_{cb}^* V_{cd}}{V_{ub}^* V_{ud}}\right) = -\arg\left(\frac{V_{ub}^* V_{ud}}{V_{cb}^* V_{cd}}\right) \\ &= \pi - \arg\left(-\frac{V_{ub}^* V_{ud}}{V_{cb}^* V_{cd}}\right) = \pi - \gamma \end{aligned} \quad (16)$$

where γ is one of the angles of the usual Unitarity Triangle UT_{db} of Fig. 1. Note also that Φ_{DCS} and Φ_{CA} are convention dependent, while $\Phi_{DCS} - \Phi_{CA}$ is not.

One then writes the decay widths $\Gamma[B^+ \rightarrow (K^-\pi^+)_{D^0}K^+]$ and $\Gamma[B^+ \rightarrow (K^-\pi^+)_{\overline{D^0}}K^+]$,

$$\Gamma[B^+ \rightarrow (K^-\pi^+)_{D^0}K^+] = |A_{DCS} + A_{CA}|^2$$

$$\Gamma[B^- \rightarrow (K^+\pi^-)_D K^-] = |\bar{A}_{DCS} + \bar{A}_{CA}|^2 \quad (17)$$

Thus, as discussed in the section above, with $\Delta = \alpha_1 - \alpha_2$, one has

$$\begin{aligned} \Gamma[B^+ \rightarrow (K^-\pi^+)_D K^+] &= a_{DCS}^2 + a_{CA}^2 + 2a_{DCS}a_{CA}[-\cos\Delta \cos\gamma - \sin\Delta \sin\gamma] \\ \Gamma[B^- \rightarrow (K^+\pi^-)_D K^-] &= a_{DCS}^2 + a_{CA}^2 + 2a_{DCS}a_{CA}[-\cos\Delta \cos\gamma + \sin\Delta \sin\gamma] \end{aligned} \quad (18)$$

where

$$\begin{aligned} a_{DCS}^2 &= \Gamma(B^+ \rightarrow \bar{D}^0 K^+) \times \Gamma(\bar{D}^0 \rightarrow K^-\pi^+) = \Gamma(B^- \rightarrow D^0 K^-) \times \Gamma(D^0 \rightarrow K^+\pi^-) \\ a_{CA}^2 &= \Gamma(B^+ \rightarrow D^0 K^+) \times \Gamma(D^0 \rightarrow K^-\pi^+) = \Gamma(B^- \rightarrow \bar{D}^0 K^-) \times \Gamma(\bar{D}^0 \rightarrow K^+\pi^-) \end{aligned} \quad (19)$$

Thus,

$$\begin{aligned} |A|^2 &= \Gamma[B^+ \rightarrow (f_i)_D K^+] = \Gamma[B^+ \rightarrow \bar{D}^0 K^+ \rightarrow f_i K^+] \\ &\times [1 + \mathcal{R}_{B \rightarrow f_i K}^2 + 2\mathcal{R}_{B \rightarrow f_i K}(-\cos\Delta_{f_i} \cos\gamma - \sin\Delta_{f_i} \sin\gamma)] \\ |\bar{A}|^2 &= \Gamma[B^- \rightarrow (f_i)_D K^-] = \Gamma[B^+ \rightarrow \bar{D}^0 K^+ \rightarrow f_i K^+] \\ &\times [1 + \mathcal{R}_{B \rightarrow f_i K}^2 + 2\mathcal{R}_{B \rightarrow f_i K}(-\cos\Delta_{f_i} \cos\gamma + \sin\Delta_{f_i} \sin\gamma)] \end{aligned} \quad (20)$$

where $f_i = K^-\pi^+$.

We rewrite equations (19) in terms of \mathcal{R} and $\mathcal{R}_{D \rightarrow f_i}$ as defined in equation (7),

$$\begin{aligned} \Gamma[B^+ \rightarrow (f_i)_D K^+] &= \Gamma[B^+ \rightarrow \bar{D}^0 K^+ \rightarrow f_i K^+] \\ &\times [1 + (\mathcal{R}\mathcal{R}_{D \rightarrow f_i})^2 + 2\mathcal{R}\mathcal{R}_{D \rightarrow f_i}(-\cos\Delta_{f_i} \cos\gamma - \sin\Delta_{f_i} \sin\gamma)] \\ \Gamma[B^- \rightarrow (\bar{f}_i)_D K^-] &= \Gamma[B^+ \rightarrow \bar{D}^0 K^+ \rightarrow f_i K^+] \\ &\times [1 + (\mathcal{R}\mathcal{R}_{D \rightarrow f_i})^2 + 2\mathcal{R}\mathcal{R}_{D \rightarrow f_i}(-\cos\Delta_{f_i} \cos\gamma + \sin\Delta_{f_i} \sin\gamma)] \end{aligned} \quad (21)$$

As discussed in the previous section, \mathcal{R} can be determined experimentally using the B^\pm using semileptonic decays of the $\bar{D}^0(D^0)$ and $\mathcal{R}_{D \rightarrow f_i}$ can be determined from the $D^{*\pm}$ decays, where the charge of the pion identifies the flavor of the D^0 meson.

Therefore γ can be extracted from equation (20) provided the total number of produced B^\pm is known in order to evaluate $\Gamma[B^+ \rightarrow \bar{D}^0 K^+ \rightarrow f_i K^+]$ following equation (12).

Should one leave $\Gamma[B^+ \rightarrow \bar{D}^0 K^+ \rightarrow f_i K^+]$ as a free parameter, we would be left with three unknowns for two equations and thus one should use additional modes. For example, one can consider the final state $\bar{f}_i = K^+\pi^-$. Using equations (21) and the relations in equation (8), one derives

$$\begin{aligned} \Gamma[B^+ \rightarrow (\bar{f}_i)_D K^+] &= \Gamma[B^+ \rightarrow \bar{D}^0 K^+ \rightarrow f_i K^+] \\ &\times [\mathcal{R}_{D \rightarrow \bar{f}_i}^2 + \mathcal{R}^2 + 2\mathcal{R}\mathcal{R}_{D \rightarrow \bar{f}_i}(-\cos\bar{\Delta}_{\bar{f}_i} \cos\gamma - \sin\bar{\Delta}_{\bar{f}_i} \sin\gamma)] \end{aligned}$$

$$\begin{aligned} \Gamma[B^- \rightarrow (f_i)_D K^-] &= \Gamma[B^+ \rightarrow \overline{D^0} K^+ \rightarrow f_i K^+] \\ &\times [\mathcal{R}_{D \rightarrow f_i}^2 + \mathcal{R}^2 + 2\mathcal{R}\mathcal{R}_{D \rightarrow f_i}(-\cos \overline{\Delta}_{\overline{f_i}} \cos \gamma + \sin \overline{\Delta}_{\overline{f_i}} \sin \gamma)] \end{aligned} \quad (22)$$

Compared to equation (20), an additional parameter, $\overline{\Delta}_{\overline{f_i}}$, has been introduced. It concerns a strong phase difference as is discussed here below. Altogether, with equations (21) and (22), we have now four parameters, $\Gamma[B^+ \rightarrow \overline{D^0} K^+ \rightarrow f_i K^+]$, Δ_{f_i} , $\overline{\Delta}_{\overline{f_i}}$ and γ , and four equations. Thus γ can be extracted.

For completeness, we write the CP asymmetries

$$\begin{aligned} \mathcal{A}_{CP}(f_i = K^- \pi^+) &= \frac{\Gamma[B^+ \rightarrow (K^- \pi^+)_D K^+] - \Gamma[B^- \rightarrow (K^+ \pi^-)_D K^-]}{\Gamma[B^+ \rightarrow (K^- \pi^+)_D K^+] + \Gamma[B^- \rightarrow (K^+ \pi^-)_D K^-]} \\ \mathcal{A}_{CP}(f_i = K^- \pi^+) &= \frac{-2\mathcal{R}\mathcal{R}_{D \rightarrow f_i} \sin \Delta_{f_i} \sin \gamma}{1 + \mathcal{R}^2 \mathcal{R}_{D \rightarrow f_i}^2 - 2\mathcal{R}\mathcal{R}_{D \rightarrow f_i} \cos \Delta_{f_i} \cos \gamma} \end{aligned} \quad (23)$$

$$\begin{aligned} \mathcal{A}_{CP}(\overline{f_i} = K^+ \pi^-) &= \frac{\Gamma[B^+ \rightarrow (K^+ \pi^-)_D K^+] - \Gamma[B^- \rightarrow (K^- \pi^+)_D K^-]}{\Gamma[B^+ \rightarrow (K^+ \pi^-)_D K^+] + \Gamma[B^- \rightarrow (K^- \pi^+)_D K^-]} \\ \mathcal{A}_{CP}(\overline{f_i} = K^+ \pi^-) &= \frac{-2\mathcal{R}\mathcal{R}_{D \rightarrow f_i} \sin \overline{\Delta}_{\overline{f_i}} \sin \gamma}{\mathcal{R}_{D \rightarrow f_i}^2 + \mathcal{R}^2 - 2\mathcal{R}\mathcal{R}_{D \rightarrow f_i} \cos \overline{\Delta}_{\overline{f_i}} \cos \gamma} \end{aligned} \quad (24)$$

Comparing equations (23) and (24), the only parameters, which differ are Δ_{f_i} and $\overline{\Delta}_{\overline{f_i}}$.

$$\begin{aligned} \Delta_{f_i} &= \zeta_{\overline{D^0}} - \zeta_{D^0} + \delta_{1_{f_i}} - \delta_{2_{f_i}} = \Delta_{\zeta} + \Delta_{\delta_{f_i}} \\ \overline{\Delta}_{\overline{f_i}} &= \zeta_{\overline{D^0}} - \zeta_{D^0} + \delta_{1_{\overline{f_i}}} - \delta_{2_{\overline{f_i}}} = \Delta_{\zeta} + \Delta_{\delta_{\overline{f_i}}} \end{aligned} \quad (25)$$

where $\zeta_{\overline{D^0}}$ is related to $B^+ \rightarrow \overline{D^0} K^+$ and ζ_{D^0} to $B^+ \rightarrow D^0 K^+$, while $\delta_{1_{f_i(\overline{f_i})}}$ is related to $\overline{D^0} \rightarrow f_i(\overline{f_i})$ and $\delta_{2_{f_i(\overline{f_i})}}$ to $D^0 \rightarrow f_i(\overline{f_i})$.

It is important to underline that in general neither of these strong phase differences Δ_{ζ} or Δ_{δ} are expected to vanish.

As a final comment, the asymmetry $\mathcal{A}_{CP}(\overline{f_i} = K^+ \pi^-)$ is expected to be very small since it suffers of a very low statistics for the mode $B^+ \rightarrow D^0 K^+ \rightarrow (K^+ \pi^-)_{D^0} K^+$, as it has multiple suppression factors compared to $B^+ \rightarrow \overline{D^0} K^+ \rightarrow (K^+ \pi^-)_{\overline{D^0}} K^+$, namely V_{ub} instead of V_{cb} , as well as color and double Cabibbo suppressions.

In the following, we will not pursue the modes $\overline{D^0}(D^0) \rightarrow K^{\pm} \pi^{\mp}$. The reason is that they do not measure directly one of the phases of the ‘‘flat’’ triangle UT_{sb} defined in (1), that is the main interest of the present paper.

2.3 Using $\overline{D^0}(D^0)$ decays to CP eigenstates

2.3.1 $\overline{D^0}(D^0)$ decays to $\pi^+\pi^-$

Let us first examine the decay $\overline{D^0}(D^0) \rightarrow \pi^+\pi^-$, i.e. $CP = +$. The complete amplitudes read

$$\begin{aligned} A_1 &= a_{\overline{D^0}(\pi\pi)} e^{i\alpha_{\overline{D^0}(\pi\pi)}} e^{i\Phi_{\overline{D^0}(\pi\pi)}} , \quad A_2 = a_{D^0(\pi\pi)} e^{i\alpha_{D^0(\pi\pi)}} e^{i\Phi_{D^0(\pi\pi)}} \\ \overline{A}_1 &= a_{\overline{D^0}(\pi\pi)} e^{i\alpha_{\overline{D^0}(\pi\pi)}} e^{-i\Phi_{\overline{D^0}(\pi\pi)}} , \quad \overline{A}_2 = a_{D^0(\pi\pi)} e^{i\alpha_{D^0(\pi\pi)}} e^{-i\Phi_{D^0(\pi\pi)}} \end{aligned} \quad (26)$$

where

$$\Phi_{\overline{D^0}(\pi\pi)} = \arg(V_{cb}^* V_{us} V_{ud}^* V_{cd}) , \quad \Phi_{D^0(\pi\pi)} = \arg(V_{ub}^* V_{cs} V_{cd}^* V_{ud}) \quad (27)$$

that gives

$$\begin{aligned} \Phi_{\overline{D^0}(\pi\pi)} - \Phi_{D^0(\pi\pi)} &= \arg\left(\frac{V_{cb}^* V_{cd}}{V_{ub}^* V_{ud}} \frac{V_{ud}^* V_{us}}{V_{cd}^* V_{cs}}\right) \\ &= \arg\left(-\frac{V_{cb}^* V_{cd}}{V_{ub}^* V_{ud}}\right) + \arg\left(-\frac{V_{ud}^* V_{us}}{V_{cd}^* V_{cs}}\right) \\ &= -\gamma + \gamma_{ds} \simeq -\gamma \end{aligned} \quad (28)$$

where γ is one of the angles of the usual Unitarity Triangle UT_{bd} , and γ_{ds} is a very small angle of the 3rd triangle UT_{ds} in formulas (1) (2) and Fig. 1.

One obtains the partial widths,

$$\begin{aligned} \Gamma[B^+ \rightarrow (\pi\pi)_D K^+] &= \Gamma[B^+ \rightarrow \overline{D^0} K^+ \rightarrow (\pi\pi) K^+] \\ &\quad \times [1 + \mathcal{R}^2 + 2\mathcal{R}(\cos \Delta \cos \gamma + \sin \Delta \sin \gamma)] \\ \Gamma[B^- \rightarrow (\pi\pi)_D K^-] &= \Gamma[B^+ \rightarrow \overline{D^0} K^+ \rightarrow (\pi\pi) K^+] \\ &\quad \times [1 + \mathcal{R}^2 + 2\mathcal{R}(\cos \Delta \cos \gamma - \sin \Delta \sin \gamma)] \end{aligned} \quad (29)$$

The asymmetry reads

$$\begin{aligned} \mathcal{A}_{CP}^+(\pi\pi) &= \frac{\Gamma[B^+ \rightarrow (\pi^+\pi^-)_D K^+] - \Gamma[B^- \rightarrow (\pi^+\pi^-)_D K^-]}{\Gamma[B^+ \rightarrow (\pi^+\pi^-)_D K^+] + \Gamma[B^- \rightarrow (\pi^+\pi^-)_D K^-]} \\ \mathcal{A}_{CP}^+(\pi\pi) &\simeq \frac{+2\mathcal{R} \sin \Delta \sin \gamma}{1 + \mathcal{R}^2 + 2\mathcal{R} \cos \Delta \cos \gamma} \end{aligned} \quad (30)$$

where \mathcal{R} is defined in equation (5) and $\Delta = \alpha_{\overline{D^0}(\pi\pi)} - \alpha_{D^0(\pi\pi)} \simeq \Delta_\zeta$. This is indeed so because $\Delta_\delta \simeq 0$ in CP eigenstate decays of D mesons.

2.3.2 $\overline{D^0}(D^0)$ decays to K^+K^-

We consider now the decays $B^+ \rightarrow D^0(\overline{D^0}) \rightarrow (K^+K^-)_D K^+$, i.e. $CP = +$. The complete amplitudes read :

$$\begin{aligned} A_1 &= a_{\overline{D^0}(KK)} e^{i\alpha_{\overline{D^0}(KK)}} e^{i\Phi_{\overline{D^0}(KK)}} , \quad A_2 = a_{D^0(KK)} e^{i\alpha_{D^0(KK)}} e^{i\Phi_{D^0(KK)}} \\ \overline{A}_1 &= a_{\overline{D^0}(KK)} e^{i\alpha_{\overline{D^0}(KK)}} e^{-i\Phi_{\overline{D^0}(KK)}} , \quad \overline{A}_2 = a_{D^0(KK)} e^{i\alpha_{D^0(KK)}} e^{-i\Phi_{D^0(KK)}} \end{aligned} \quad (31)$$

where the CP phases read

$$\Phi_{\overline{D^0}(KK)} = \arg(V_{cb}^* V_{cs}) , \quad \Phi_{D^0(KK)} = \arg(V_{ub}^* V_{us}) \quad (32)$$

$$\Phi_{\overline{D^0}(KK)} - \Phi_{D^0(KK)} = \arg\left(\frac{V_{cb}^* V_{cs}}{V_{ub}^* V_{us}}\right) = \pi + \gamma_s \quad (33)$$

The angle γ_s is one of the angles of the Unitarity Triangle UT_{sb} in Fig. 1.

One obtains the partial widths from equation (21),

$$\begin{aligned} \Gamma[B^+ \rightarrow (K^+K^-)_D K^+] &= \Gamma[B^+ \rightarrow \overline{D^0} K^+ \rightarrow (K^+K^-) K^+] \\ &\quad \times [1 + \mathcal{R}^2 + 2\mathcal{R}(-\cos \Delta \cos \gamma_s + \sin \Delta \sin \gamma_s)] \\ \Gamma[B^- \rightarrow (K^+K^-)_D K^-] &= \Gamma[B^+ \rightarrow \overline{D^0} K^+ \rightarrow (K^+K^-) K^+] \\ &\quad \times [1 + \mathcal{R}^2 + 2\mathcal{R}(-\cos \Delta \cos \gamma_s - \sin \Delta \sin \gamma_s)] \end{aligned} \quad (34)$$

The asymmetry reads

$$\begin{aligned} \mathcal{A}_{CP}^+(K^+K^-) &= \frac{\Gamma[B^+ \rightarrow (K^+K^-)_D K^+] - \Gamma[B^- \rightarrow (K^+K^-)_D K^-]}{\Gamma[B^+ \rightarrow (K^+K^-)_D K^+] + \Gamma[B^- \rightarrow (K^+K^-)_D K^-]} \\ \mathcal{A}_{CP}^+(K^+K^-) &= \frac{+2\mathcal{R} \sin \Delta \sin \gamma_s}{1 + \mathcal{R}^2 - 2\mathcal{R} \cos \Delta \cos \gamma_s} \end{aligned} \quad (35)$$

where \mathcal{R} is defined in equation (7) and $\Delta = \alpha_{\overline{D^0}(KK)} - \alpha_{D^0(KK)} \simeq \Delta_\zeta$.

A similar result is obtained with the decay $\overline{D^0}(D^0) \rightarrow K_s \pi^0$. However due to the different CP sign ($\eta_{CP} = -1$) for the eigenstate $K_s \pi^0$, the CP asymmetry reads

$$\mathcal{A}_{CP}^-(K_s \pi^0) = \frac{-2\mathcal{R} \sin \Delta \sin \gamma_s}{1 + \mathcal{R}^2 + 2\mathcal{R} \cos \Delta \cos \gamma_s} \quad (36)$$

with $\Delta_{K_s \pi^0} = \alpha_{\overline{D^0}(K_s \pi^0)} - \alpha_{D^0(K_s \pi^0)} \simeq \Delta_\zeta$.

Using Eqns. (35) and (36) one can extract $\Delta (= \Delta_\zeta)$ and γ_s . This method had been proposed by Gronau, London and Wyler [5] for the determination of the angle γ , since $\gamma_s \simeq -\gamma$, up to a very small correction. However, we are now interested in the angle γ_s of the UT_{sb} unitarity triangle. Indeed, one gets

$$\sin \Delta \sin \gamma_s = \frac{\mathcal{A}_{CP}^-(K_s \pi^0) \times \mathcal{A}_{CP}^+(K^+K^-)}{\mathcal{A}_{CP}^-(K_s \pi^0) - \mathcal{A}_{CP}^+(K^+K^-)} \times \frac{1 + \mathcal{R}^2}{\mathcal{R}}$$

$$\cos \Delta \cos \gamma_s = -\frac{\mathcal{A}_{CP}^-(K_s \pi^0) + \mathcal{A}_{CP}^+(K^+ K^-)}{\mathcal{A}_{CP}^-(K_s \pi^0) - \mathcal{A}_{CP}^+(K^+ K^-)} \times \frac{1 + \mathcal{R}^2}{2\mathcal{R}} \quad (37)$$

Thus γ_s can be measured, though in general with a 8-fold ambiguity. However depending upon the values of \mathcal{A}_{CP}^+ and \mathcal{A}_{CP}^- some solutions may not be physical and thus the ambiguities reduced. Several other $CP = -$ modes can be used to increase statistics, such as $\overline{D}^0(D^0) \rightarrow K_s \eta(\eta')$ or $K_s \omega$.

2.4 Convention of the difference of strong phases

Here we comment on our convention on the difference of the strong phases Δ_{f_i} , that differs from the convention in other works. Let us just consider the particular case of $B^\pm \rightarrow D^0(\overline{D}^0)K^\pm$, as made very explicit by Gronau [6].

Let us compare the notation of our amplitudes

$$A[B^+ \rightarrow \overline{D}^0 K^+] = a_1 e^{i\alpha_1} e^{i\Phi_1}, \quad A[B^+ \rightarrow D^0 K^+] = a_2 e^{i\alpha_2} e^{i\Phi_2} \quad (38)$$

and the CP-conjugated ones,

$$A[B^- \rightarrow D^0 K^-] = a_1 e^{i\alpha_1} e^{-i\Phi_1}, \quad A[B^- \rightarrow \overline{D}^0 K^-] = a_2 e^{i\alpha_2} e^{-i\Phi_2} \quad (39)$$

with Gronau convention, his formula (4),

$$A[B^- \rightarrow D^0 K^-] = |A|, \quad A[B^- \rightarrow \overline{D}^0 K^-] = |\overline{A}| e^{i\delta} e^{-i\gamma} \quad (40)$$

and its CP-conjugated,

$$A[B^+ \rightarrow \overline{D}^0 K^+] = |A|, \quad A[B^+ \rightarrow D^0 K^+] = |\overline{A}| e^{i\delta} e^{i\gamma} \quad (41)$$

One has

$$\delta = \alpha_2 - \alpha_1 = -\Delta, \quad \Phi_2 - \Phi_1 = -\Phi = \gamma \quad (42)$$

and finally

$$\Delta = -\delta, \quad \Phi = \Phi_1 - \Phi_2 = -\gamma \quad (43)$$

So our FSI phase has the opposite sign to Gronau convention, and the CKM phase is the same in both conventions. The convention of Gronau is the same as the one used by HFAG [7], where the phase δ is denoted by δ_B . The opposite sign also holds for our general strong phase difference Δ_{f_i} and the one of HFAG $\delta_B + \delta_D$.

3 Estimating the size of the modulus of amplitudes

The ratio of amplitudes can be extracted experimentally from the measured branching fraction (see Table 1).

Mode	Br	η_{CP}	\mathcal{R}	$\mathcal{R}_{D \rightarrow f_i}$
$B^+ \rightarrow \overline{D^0}K^+$	$(3.63 \pm 0.12) \cdot 10^{-4}$			-
$B^+ \rightarrow D^0K^+$	$(3.57 \pm 0.35) \cdot 10^{-6}$		0.099 ± 0.005	-
$B^+ \rightarrow \overline{D^0}K^{*+}$	$(5.3 \pm 0.4) \cdot 10^{-4}$			-
$B^+ \rightarrow D^0K^{*+}$	$(3.1 \pm 1.6) \cdot 10^{-6}$		0.076 ± 0.020	-
$\overline{D^0} \rightarrow K^+\pi^-$	$(3.950 \pm 0.031) \cdot 10^{-2}$		-	0.0616 ± 0.0015
$\overline{D^0} \rightarrow K^-\pi^+$	$(1.50 \pm 0.07) \cdot 10^{-4}$		-	16.23 ± 0.38
$\overline{D^0} \rightarrow \pi^+\pi^-$	$(1.455 \pm 0.024) \cdot 10^{-3}$	+1	-	1
$\overline{D^0} \rightarrow K^+K^-$	$(4.08 \pm 0.06) \cdot 10^{-3}$	+1	-	1
$\overline{D^0} \rightarrow K_s\pi^0$	$(1.240 \pm 0.022) \cdot 10^{-2}$	-1	-	1
$\overline{D^0} \rightarrow K_s\eta$	$(5.090 \pm 0.013) \cdot 10^{-3}$	-1	-	1
$\overline{D^0} \rightarrow K_s\eta'$	$(9.49 \pm 0.32) \cdot 10^{-3}$	-1	-	1
$\overline{D^0} \rightarrow K_s\omega$	$(1.11 \pm 0.06) \cdot 10^{-2}$	-1	-	1

Table 1. The branching fraction of B^+ decays to final states $\overline{D^0}(D^0)K^+(K^{*+})$ and the subsequent $\overline{D^0}(D^0)$ decays [4].

Using the measured Branching Fractions [4], one gets :

$$\mathcal{R} = \sqrt{\frac{Br(B^+ \rightarrow D^0K^+)}{Br(B^+ \rightarrow \overline{D^0}K^+)}} = 0.099 \pm 0.005 \quad (44)$$

$$\mathcal{R}_{D \rightarrow K^-\pi^+} = \sqrt{\frac{Br(D^0 \rightarrow K^-\pi^+)}{Br(\overline{D^0} \rightarrow K^-\pi^+)}} = 16.23 \pm 0.38 \quad (45)$$

$$\mathcal{R}_{B \rightarrow (K^-\pi^+)K} = \mathcal{R} \times \mathcal{R}_{D \rightarrow K^-\pi^+} = 1.609 \pm 0.092$$

For any CP -eigenstate, such as $f_{CP} = \pi^+\pi^-$, K^+K^- or $K_s\pi^0$, $\mathcal{R}_{B \rightarrow (f_{CP})DK} = \mathcal{R}$. Indeed, in the former equation, $\frac{Br[D^0 \rightarrow CP_{eigenstate}]}{Br[\overline{D^0} \rightarrow CP_{eigenstate}]} = 1$ is assumed, since $|D_{CP\pm}^0\rangle = \frac{1}{\sqrt{2}}[|D^0\rangle \pm |\overline{D^0}\rangle]$.

As already mentioned in section 2.1, the ratio $Br(B^+ \rightarrow D^0K^+)/Br(B^+ \rightarrow \overline{D^0}K^+)$ should be measured even much more precisely at FCCee from the decays $B^+ \rightarrow D^0K^+ \rightarrow \ell^+\nu K^-K^+$ and $B^+ \rightarrow \overline{D^0}K^+ \rightarrow \ell^-\bar{\nu}K^+K^+$. The respective branching fractions are about $1.26 \cdot 10^{-7}$ and $1.29 \cdot 10^{-5}$. With the statistics expected at FCCee, one gets $5 \cdot 10^4$ and $5 \cdot 10^6$ events, respectively. Despite background levels orders of magnitude larger, it should be possible to extract the signal rather cleanly thanks to very accurate vertexing and particle identification for the kaons. A precision on $\delta(\mathcal{R})/\mathcal{R}$ at the level of $5 \cdot 10^{-3}$ seems attainable.

4 Expected Asymmetry Sensitivities at FCCee

In this section, we investigate the sensitivity on γ_s , which one may expect at FCCee. The expected number of events at summarized in Table 2.

$\sigma(e^+e^- \rightarrow Z)$ nb	number of Z	$E_{\text{cm}} = 91.2 \text{ GeV}$ and $\int L = 150\text{ab}^{-1}$ $f(Z \rightarrow B^+)$	Number of produced B^+
~ 42.9	$\sim 6.4 \cdot 10^{12}$	~ 0.061	$\sim 3.9 \cdot 10^{11}$

B^+ decay Mode	Decay Mode	Final State	Number of B^+ decays
$\overline{D}^0/D^0 \rightarrow \text{nonCP eigenstates}$			
$\overline{D}^0 K^+$	$\overline{D}^0 \rightarrow K^+ \pi^-$	$K^+ \pi^- K^+$	$\sim 5.6 \cdot 10^6$
$\overline{D}^0 K^+$	$\overline{D}^0 \rightarrow K^- \pi^+$	$K^- \pi^+ K^+$	$\sim 2.1 \cdot 10^4$
$D^0 K^+$	$D^0 \rightarrow K^- \pi^+$	$K^- \pi^+ K^+$	$\sim 5.5 \cdot 10^4$
$D^0 K^+$	$D^0 \rightarrow K^+ \pi^-$	$K^+ \pi^- K^+$	$\sim 2.1 \cdot 10^2$
$\overline{D}^0/D^0 \rightarrow \text{CP eigenstates}$			
$\overline{D}^0 K^+$	$\overline{D}^0 \rightarrow \pi^+ \pi^-$	$\pi^+ \pi^- K^+$	$\sim 2.1 \cdot 10^5$
$D^0 K^+$	$D^0 \rightarrow \pi^+ \pi^-$	$\pi^+ \pi^- K^+$	$\sim 2.0 \cdot 10^3$
$\overline{D}^0 K^+$	$\overline{D}^0 \rightarrow K^+ K^-$	$K^+ K^- K^+$	$\sim 5.8 \cdot 10^5$
$D^0 K^+$	$D^0 \rightarrow K^+ K^-$	$K^+ K^- K^+$	$\sim 5.7 \cdot 10^3$
$\overline{D}^0 K^+$	$\overline{D}^0 \rightarrow K_s \pi^0$	$K_s \pi^0 K^+$	$\sim 1.2 \cdot 10^6$
$D^0 K^+$	$D^0 \rightarrow K_s \pi^0$	$K_s \pi^0 K^+$	$\sim 1.2 \cdot 10^4$
$\overline{D}^0 K^+$	$\overline{D}^0 \rightarrow K_s \eta$	$K_s \eta K^+$	$\sim 5.0 \cdot 10^5$
$D^0 K^+$	$D^0 \rightarrow K_s \eta$	$K_s \eta K^+$	$\sim 4.9 \cdot 10^3$
$\overline{D}^0 K^+$	$\overline{D}^0 \rightarrow K_s \eta'$	$K_s \eta' K^+$	$\sim 9.3 \cdot 10^5$
$D^0 K^+$	$D^0 \rightarrow K_s \eta'$	$K_s \eta' K^+$	$\sim 9.1 \cdot 10^3$
$\overline{D}^0 K^+$	$\overline{D}^0 \rightarrow K_s \omega$	$K_s \omega K^+$	$\sim 1.1 \cdot 10^6$
$D^0 K^+$	$D^0 \rightarrow K_s \omega$	$K_s \omega K^+$	$\sim 1.1 \cdot 10^4$

Table 2. The mean expected number of produced B^+ decays to specific decay modes at FCCee at a center of mass energy of 91 GeV over 5 years with 2 detectors. These numbers have to be multiplied by 2 when including B^- decays. The branching fractions of the PDG [4] have been used (only the K_s decay to $\pi^+ \pi^-$ is included). Note that the number of events is indicative since the exact numbers depend on the value of the strong phase differences (Δ) and the CKM phases involved, as seen in eqn. (4).

4.1 Generic Detector acceptance and resolutions

We define below a generic detector, the resolutions of which are parametrized as follow :

$$\begin{aligned}
 & \text{Acceptance : } |\cos \theta| < 0.95 \\
 & \text{Track } p_T \text{ resolution : } \frac{\sigma(p_T)}{p_T^2} = 2. \times 10^{-5} \oplus \frac{1.2 \times 10^{-3}}{p_T \sin \theta} \\
 & \text{Track } \phi, \theta \text{ resolution : } \sigma(\phi, \theta) \text{ } \mu\text{rad} = 18 \oplus \frac{1.5 \times 10^3}{p_T \sqrt[3]{\sin \theta}} \\
 & \text{Vertex resolution : } \sigma(d_{\text{Im}}) \text{ } \mu\text{m} = 1.8 \oplus \frac{5.4 \times 10^1}{p_T \sqrt{\sin \theta}} \quad (46) \\
 & \text{Vertex resolution : } \langle \sigma(d_{\text{Im}}) \rangle \text{ bachelor K in } D_s K \\
 & \quad \langle \sigma(d_{\text{Im}}) \rangle \simeq 10 \text{ } \mu\text{m} \\
 & \text{Calorimeter resolution : } \frac{\sigma(E)}{E} = \frac{3 \times 10^{-2}}{\sqrt{E}} \oplus 5 \times 10^{-3}
 \end{aligned}$$

where θ, ϕ are the track polar and azimuthal angle respectively, p_T (in GeV) the track transverse momentum, E the e^\pm, γ energy and d_{Im} the impact parameter. Although the tracking resolutions can be obtained with a combination of silicon vertex detector and a gaseous central tracking system, the calorimeter resolution requires a crystal type detector.

The decays $B^+ \rightarrow \overline{D^0}(D^0)K^+ \rightarrow (K^+K^-)_D K^+$ and $B^+ \rightarrow \overline{D^0}(D^0)K^+ \rightarrow (K_s \pi^0)_D K^+$ have then been simulated using the resolutions in Equations (46).

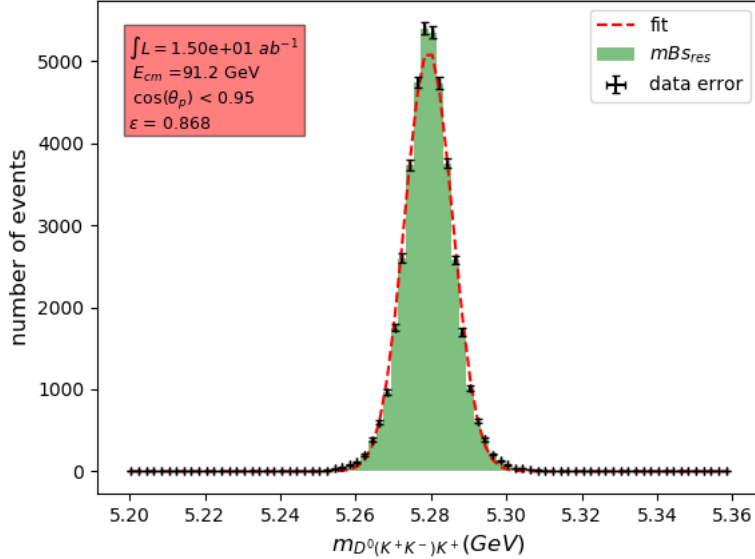


Fig. 4. The B^\pm resolutions for the D decays K^+K^- in $e^+e^- \rightarrow Z \rightarrow B^+ \rightarrow D^0 K^+ \rightarrow K^+ K^- K^+$.

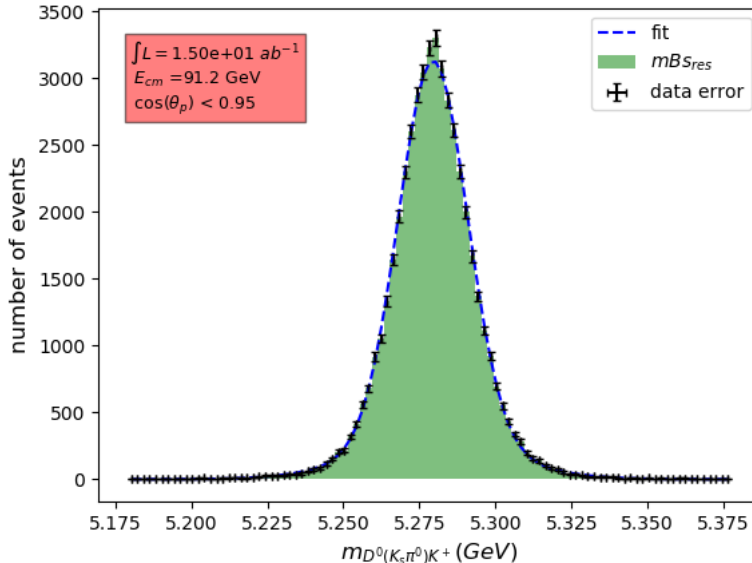


Fig. 5. The B^\pm resolutions for the D decays $K_s\pi^0$ in $e^+e^- \rightarrow Z \rightarrow B^\pm \rightarrow D^0 K^\pm \rightarrow K_s\pi^0 K^\pm \rightarrow \pi^+\pi^-\gamma\gamma K^\pm$.

As one can see from Figs. 4 and 5, the B^\pm mass resolution is 6.4 MeV and 12.0 MeV for the $K^+K^-K^\pm$ and $K_s\pi^0K^\pm$ final states, respectively. For the latter decay, we use the constraint of the D^0 mass, which improves significantly the resolution. However, this resolution should worsen with a complete simulation, which will include accurately the flight distances of the resonances B^\pm , D^0 and K_s . It can also be noted that, using the values $\Delta = -130^\circ$ and $\gamma_s = 108^\circ$, one gets about the same number of events for both modes within 30%, once the acceptances are taken into account, in particular when requiring the K_s to decay within a fiducial volume of $r = 1$ meter in the transverse direction and $z = \pm 1$ meter in the longitudinal direction. Such a fiducial volume for K_s reconstruction implies that the tracking volume of the detector should be large enough, e.g. $r_{det.} > 2$ meter, $z_{det.} > \pm 2$ meter to enable efficient reconstruction of the $\pi^+\pi^-$ pair. The tracking system should also consist of a large number of measurement layers, as shown in the appendix, which presents an experimental study of the performance of K_s reconstruction in a FCC-ee detector. As a final comment, one should note that in order to keep the background at a negligible level, an efficient particle identification system is required enabling to identify the kaons in a wide range from $\sim 1 - 30$ GeV.

4.2 Sensitivity on the CKM angle γ_s

To study the sensitivity, we assume a specific case with $\Delta = -130^\circ$ and $\gamma_s = 108^\circ$. With these figures, the asymmetries $A_{CP}^+(K^+K^-)$ and $A_{CP}^-(K_s\pi^0)$, as defined in equations (35) and (36) are -0.1489 and 0.1377, respectively.

Using the expected number of events for the mode $B^\pm \rightarrow (K^+K^-)_D K^\pm$ and $B^\pm \rightarrow (K_s\pi^0)_D K^\pm$, and for a total integrated luminosity of $150 ab^{-1}$ accumulated by the addition of all experiments at FCCee, the expected sensitivity for $\delta(\gamma_s)$ is about 2.7° if $\Delta = -130^\circ$. Such a value for Δ corresponds to the

strong phase in the decay $B^+ \rightarrow D^0 K^+$ as has been measured, and reported in [4], $\delta_B = 130^\circ$, taking into account our convention $\Delta = -\delta_B$, as exposed in section 2.4.

One should note that the γ_s sensitivity can vary according to the actual value of the strong angle difference Δ , as can be seen in Table 3. The most favourable situation occurs when $\Delta = -90^\circ$, in which case $\delta(\gamma_s) \simeq 0.8^\circ$. When $\Delta = \pm\gamma_s$, the first equation in (37) determines the sine-squared of this common (modulo the sign) angle, and is redundant with the second equation of (37), which determines the cosine-squared. Consequently, the equations (37) do not allow a simultaneous extraction of the angles Δ and γ_s . The same applies when $\Delta = 180^\circ \pm \gamma_s$. In the vicinity of these singularities, the experimental uncertainties on $\mathcal{A}_{CP}^+(K^+K^-)$ and on $\mathcal{A}_{CP}^-(K_s\pi^0)$ cause equation (37) to not always have real solutions – for example, that would happen with a probability larger than 30% when the angles are within 8° of a singularity. These cases are not considered in Table 3.

These results can be improved further should one use additional $\overline{D^0}(D^0)$ CP eigenstates such as $K_s\eta$, $K_s\eta'$, $K_s\omega\dots$ and using the mode $B^\pm \rightarrow D_{CP}K^{*\pm}$ such that a sensitivity in the range 1° - 2° does not seem out of reach. Combining this with the possible direct measurements of α_s and β_s with the modes $B_s \rightarrow D_s^\pm K^\mp$ and $B_s \rightarrow J/\psi\phi$, respectively, with the expected sensitivities [1] $\delta(\alpha_s) \simeq 0.4^\circ$ and $\delta(\beta_s) \simeq 0.04^\circ$, one would directly measure the three angles of the Unitarity Triangle UT_{sb} at FCCee, without assuming the unitarity of the CKM matrix.

Δ	$\mathcal{A}_{CP}^+(K^+K^-)$	$\mathcal{A}_{CP}^-(K_s\pi^0)$	$\delta(\gamma_s)$
-10°	-0.0306	0.0345	$\sim 6.5^\circ$
-30°	-0.0887	0.0986	$\sim 2.8^\circ$
-50°	-0.1377	0.1489	$\sim 2.8^\circ$
-90°	-0.1868	0.1868	$\sim 0.8^\circ$
-120°	-0.1668	0.1570	$\sim 2.8^\circ$
-130°	-0.1489	0.1377	$\sim 2.8^\circ$
-150°	-0.0986	0.0887	$\sim 2.8^\circ$
-170°	-0.0345	0.0306	$\sim 6.5^\circ$

Table 3. The experimental sensitivity for measuring the angle γ_s at FCCee using the $B^\pm \rightarrow (K^+K^-)_D K^\pm$ and $B^\pm \rightarrow (K_s\pi^0)_D K^\pm$ decays for different values of the strong phase difference Δ . The value $\gamma_s = 108^\circ$ has been used. Finally, one notes that should one use positive values for Δ , all asymmetries will have opposite signs, but the sensitivities will remain the same.

5 Conclusion

We have investigated in this paper the sensitivity at FCCee of the angle γ_s of the Unitarity Triangle UT_{sb} , defined in Fig. 3. This result is complementary to

the ones obtained for the other angles of this triangle (α_s and β_s), as discussed in ref. [1]. Altogether, FCCee should allow one to measure directly all the angles of the rather flat Unitarity Triangle UT_{sb} , constraining further the CP sector of the Standard Model.

Appendix: reconstruction of $K_s \rightarrow \pi^+\pi^-$ decays

The measurement of the decay $B^+ \rightarrow \overline{D^0}(D^0)K^+ \rightarrow (K_s(\rightarrow \pi^+\pi^-)\pi^0)K^+$ requires an efficient reconstruction of $K_s \rightarrow \pi^+\pi^-$ decays, up to typically one meter from the interaction point (IP). This reconstruction, in a FCC-ee detector, has been studied using Monte-Carlo events that were passed through a fast simulation of the tracking system of the experiment based on DELPHES [8], and subsequently analysed within the FCCAnalyses framework [9]. The PYTHIA8 Monte-Carlo generator was used to simulate the production of $b\bar{b}$ events at $\sqrt{s} = 91.2$ GeV, in which one b quark hadronises into a charged B meson that decays into the mode of interest, while the other b -leg fragments and decays inclusively. The decay chain of the B^\pm mesons was performed with the EVTGEN program. The resulting charged particles were turned into simulated tracks using a fast tracking software implemented in DELPHES. It relies on a full description of the tracker geometry - the vertex detector and the drift chamber of the IDEA detector [10], which provide resolutions similar to the ones given in Section 4.1, being used here. The software accounts for the finite detector resolution and for the multiple scattering in each tracker layer and determines the (non diagonal) covariance matrix of the helix parameters that describe the trajectory of each charged particle. This matrix is then used to produce a smeared 5-parameters track, for each charged particle emitted within the angular acceptance of the tracker.

The reconstruction of $K_s \rightarrow \pi^+\pi^-$ heavily relies on the reconstruction of displaced vertices. Here, a standalone code is used to fit a given set of tracks to a common vertex [11], under the assumption that the trajectories be perfect helices: the track parameters are varied according to their covariance matrix so that the tracks can meet at a common point, and the vertex coordinates (x, y, z) , together with their covariance matrix, are obtained from a χ^2 minimisation. The vertexing program [11] offers the possibility to “guide” the first iteration of the fit by providing a guessed value of the radial position of the vertex, which can be inferred from the radial positions of the innermost hit of all the fitted tracks. This functionality is particularly useful when fitting tracks that made no hit in the ultra-precise silicon layers of the vertex detector surrounding the beam-pipe.

Description of the algorithm

The first step in the K_s reconstruction consists in finding the primary vertex and the primary tracks attached to this vertex (and consequently, the “secondary” tracks which will be used to search for K_s candidates). The identification of the primary vertex and of the primary tracks follows closely the LCFI+ algorithm [12]. All tracks that have been reconstructed are first fitted to a common vertex, using the knowledge of the beam-spot as an external constraint.

The track which gives the largest contribution to the χ^2 of the fit, if this contribution is larger than a given cut (here set to 25), is then removed from the list of tracks, and the vertex fit is run again. This procedure is iterated until the contribution of all tracks to the χ^2 is below the cut, providing the primary vertex and the “primary” tracks attached to it. The tracks that are not attached to the primary vertex are labelled as “secondary tracks”. This selection of secondary tracks has a typical purity of more than 97%, and is very efficient for tracks that come from a K_s decay, in the decay chain considered here.

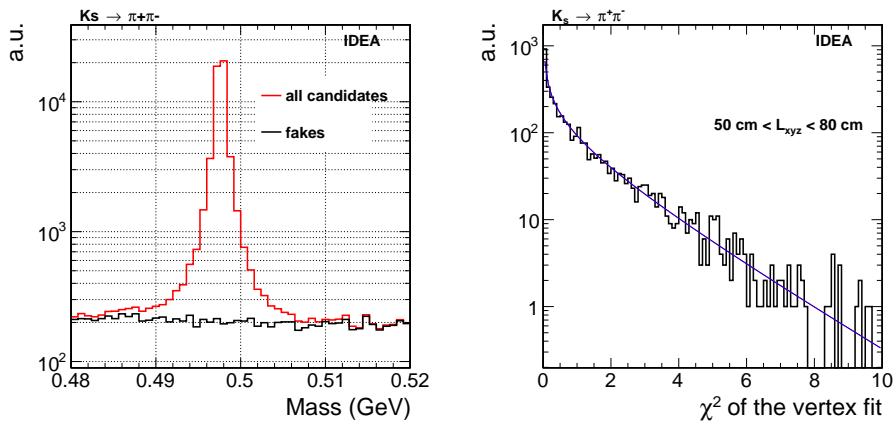


Fig. 6. Distribution of the mass of reconstructed K_s candidates in $Z \rightarrow b\bar{b}$ events which contain a $B^+ \rightarrow (K_s\pi^0)_D K^+$ decay, for all candidates (red histogram) and for fake candidates only (black histogram). Right: Distribution of the χ^2 of the vertex fit of reconstructed candidates, that are matched to a genuine K_s that decays at a distance between 50 cm and 80 cm from the interaction point. The overlaid curve represents a χ^2 function with one degree of freedom (the number of degrees of freedom of the two-tracks fit being equal to one).

The identified secondary tracks are used in the second step of the algorithm. All combinations of two opposite charge tracks are built to form K_s candidates. For each combination, the two tracks are fitted to a common vertex, and the momenta of the tracks at this vertex are used to reconstruct the mass M of the candidate, assigning the pion mass to each leg. Candidates are kept if they fulfil the loose mass cut $0.48 < M < 0.52$ GeV, and if the χ^2 of the vertex fit is smaller than 10. The latter requirement selects more than 99.4% of the K_s decays in the process of interest. The association of the reconstructed tracks to the Monte-Carlo particles is then used to determine whether a candidate is matched to a $K_s \rightarrow \pi^+\pi^-$ decay (any K_s being considered here, not necessarily the one produced in the $B^+ \rightarrow DK^+$ decay). By definition, fake candidates are those which are not matched to such a decay. The mass distribution of all K_s candidates reconstructed in the $B^+ \rightarrow DK^+$ sample, that satisfy the loose cuts listed above, is shown in Fig. 6 left. A clear peak is observed at the nominal K_s mass used in the Monte-Carlo, on top of a flat background of fake candidates. A fit of the mass distribution of genuine K_s candidates by a sum of two Gaussian functions leads to a mass resolution of about 400 keV when the

K_s decays within 30 cm from the interaction point, reaching 1 to 1.2 MeV for K_s that decay at more than 1 m from the IP. The distribution of the χ^2 of the vertex fit for candidates that are matched to a $K_s \rightarrow \pi^+\pi^-$ decay occurring in the middle of the drift chamber is shown in Fig. 6 right. It can be seen that the vertex fit behaves well, even for far detached vertices.

Kaon reconstruction efficiency

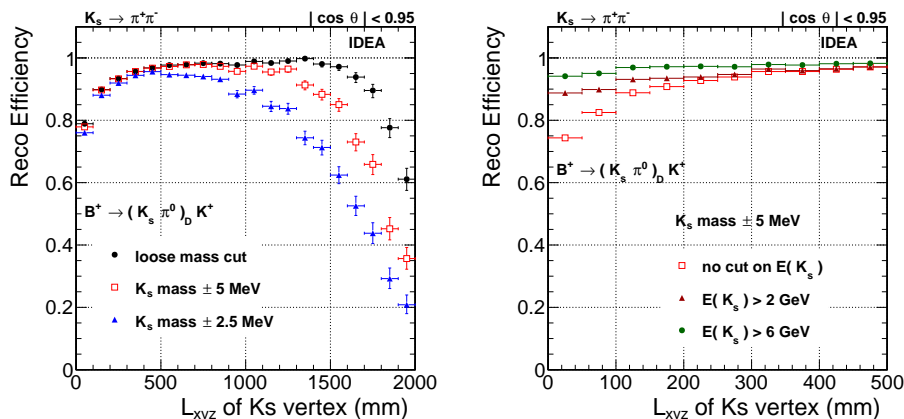


Fig. 7. Reconstruction efficiency of kaons from the $B^+ \rightarrow (K_s \pi^0)_D K^+$ decay, as a function of the distance L_{xyz} of the decay vertex of the K_s to the IP, for (left) several cuts on the K_s mass candidate, and (right) focusing on $L_{xyz} < 50$ cm and defining the efficiency with respect to kaons above a given energy.

The reconstruction efficiency is shown in Fig. 7 left, as a function of the distance L_{xyz} of the decay vertex of the K_s to the interaction point. The efficiency is defined with respect to the K_s that come from the $B^+ \rightarrow (K_s \pi^0)_D K^+$ decay, for which the Monte-Carlo daughter pions satisfy the acceptance cut $|\cos \theta| < 0.95$. The efficiency obtained with a tighter mass cut of ± 5 MeV or ± 2.5 MeV around the nominal K_s mass, which is in line with the exquisite resolution mentioned previously, is also shown. The overall efficiency amounts to 90%, 88.5% or 85% depending on the mass cut. With a cut of ± 5 MeV, the efficiency remains above 80% as long as the K_s decays within 1.5 m from the interaction point. At larger distances, the efficiency drops since the pion tracks only go through a small distance in the tracker. The drop in efficiency observed at small flight distances is due to the correlation of the flight distance with the K_s momentum: the pion tracks from K_s that decay close to the IP are softer and are more affected by multiple scattering or may lead to “loopers”. This correlation is illustrated in Fig. 7 right, which shows the efficiency to reconstruct kaons above a given energy. The small remaining inefficiency for energetic kaons that decay close to the interaction point is due to the occasional mis-assignment of the pion tracks to the primary vertex.

Purity of the K_s selection

The purity P of the K_s selection is studied in an inclusive sample of Z bosons that decay hadronically. By definition, $1 - P$ corresponds to the fraction of reconstructed K_s that are not matched to a Monte-Carlo $K_s \rightarrow \pi^+\pi^-$. Figure 8 shows this fraction of mis-identified K_s , $1 - P$, as a function of the distance L_{xyz} of the decay vertex of the K_s candidate to the interaction point. The purity is shown for two different mass cuts. Since the IDEA detector will provide a powerful identification of charged hadrons*, the purity is also shown under the assumption that charged pions can be perfectly separated from kaons and protons. At $L_{xyz} < 3$ cm, mis-identified K_s usually correspond to random combinations of tracks coming from the decays of ρ , ω , D or other mesons (in 70% of the cases, the two legs of the K_s candidate do not come from the same parent). As expected, for candidates that decay within 1 cm from the interaction point (first bin of Fig. 8 left), the purity is low, with a contamination of at least 25%. This contamination is drastically reduced as soon as the K_s candidates decay at more than 1 or 2 cm from the IP, and this requirement can easily be applied in a K_s selection as it is very efficient†. Above 3 cm, the fraction of mis-identified K_s is at the per-mil level. In 85% of the cases (98% at $L_{xyz} > 50$ cm), the two legs of the remaining fake candidates come from the same parent, and they usually correspond to Λ baryons that decay into a proton and a pion. The Λ lifetime being larger than that of the K_s , this explains the rise of the contamination with L_{xyz} , when particle identification (PID) is not used in the K_s identification, as shown in Fig. 8 right. However, this contamination is easily and efficiently suppressed by PID.

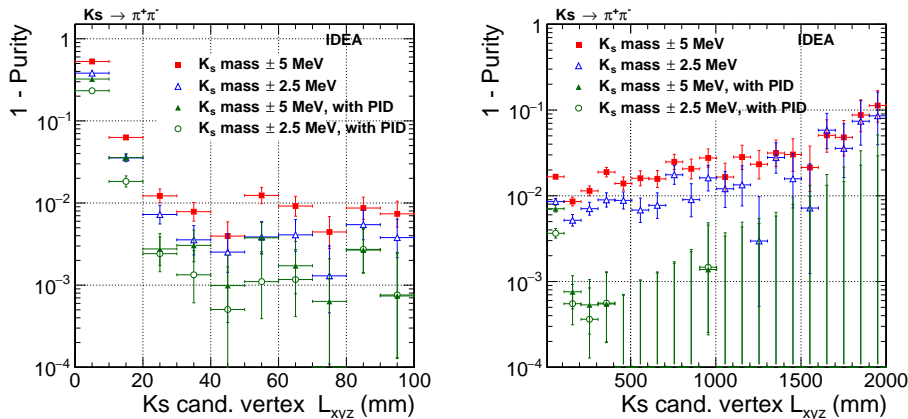


Fig. 8. Fraction of mis-identified K_s in an inclusive $Z \rightarrow$ hadrons sample, as a function of the distance L_{xyz} of the decay vertex of the candidate K_s to the IP, for (left) $0 < L_{xyz} < 10$ cm, and (right) for $1 \text{ cm} < L_{xyz} < 2$ m. The different symbols correspond to different cuts used in the K_s identification.

*This identification will be provided by measurements of the ionisation energy loss along the tracks, in the drift chamber, and by the measurement of the time-of-flight of particles, for example in a dedicated layer outside the drift chamber.

†For example, kaons from $B^+ \rightarrow (K_s \pi^0)_D K^+$ in $Z \rightarrow b\bar{b}$ events decay at more than 1 cm (2 cm) from the IP in more than 97% (94%) of the cases.

Performance in a Full Silicon tracker

A “continuous tracking”, with a very large number of layers, as is the case in a drift chamber, is clearly a key for an efficient $K_s \rightarrow \pi^+\pi^-$ reconstruction. To illustrate this point, the $B^+ \rightarrow (K_s\pi^0)_D K^+$ events used above have been processed through a simulation of the CLD detector [13]. The vertex detector of CLD is quite similar to the one of the IDEA detector, but its main tracker consists of a few layers of silicon sensors (for example six layers in the central region). Tracks made of at least five or four hits in the full tracker are used in the K_s reconstruction algorithm described above. The resulting efficiencies are shown in Fig. 9. As expected, the performance dramatically worsens compared to the efficiency shown in Fig. 7 left. One clearly sees steps corresponding to the positions of the tracker layers. For example, as there are only four barrel layers at a radial distance larger than 40 cm, the efficiency for selecting 5-hits tracks displaced by more than 40 cm vanishes in the central region, explaining the step seen in Fig. 9 left. Some efficiency can be recovered by loosening the requirement on the minimum number of hits of the tracks to four, as shown in Fig. 9 right, at the expense of a likely increased rate of fake tracks[‡]. Moreover, for K_s that decay within a few tens of centimeters from the IP, the efficiency is also lower than the one obtained with the IDEA drift chamber. This is because the material of the full silicon tracker is twice larger than the one of the IDEA tracker (drift chamber + vertex detector), leading to much larger effects from multiple scattering and worse resolutions on the K_s vertex and on the K_s mass. While some optimisations could be made to the CLD tracker, it is clear that an efficient reconstruction of $K_s \rightarrow \pi^+\pi^-$ (and of long-lived particles in general) calls for a highly transparent tracker with a very large number of layers.

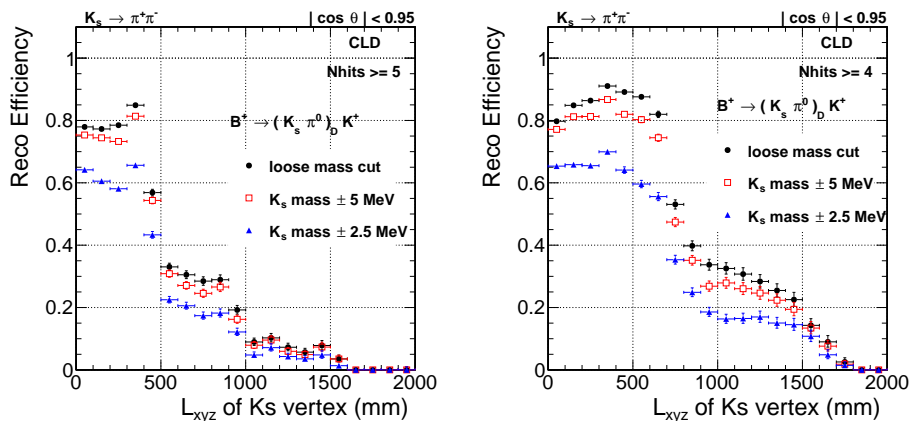


Fig. 9. Reconstruction efficiency of K_s from the $B^+ \rightarrow (K_s\pi^0)_D K^+$ decay, as a function of the distance to the IP of the decay vertex of the K_s , using tracks reconstructed in the CLD full silicon tracker, demanding at least five hits (left) or at least four hits (right) on the tracks.

[‡]Fake tracks can not be studied with the fast simulation tool used here.

Acknowledgments

We wish to thank Franco Bedeschi for making his vertexing code available and for very useful discussions about the reconstruction of far displaced vertices.

References

- [1] R. Aleksan, L. Oliver and E. Perez, arXiv:2107.02002 [hep-ph] (2021).
- [2] R. Aleksan, B. Kayser and D. London, Phys. Rev. Lett. **73** (1994) 18.
- [3] D. Atwood, I. Dunietz and A. Soni, Phys. Rev. Lett. **78** (1997) 3257.
- [4] P.A. Zyla et al. [Particle Data Group], Prog. Theor. Exp. Phys. (2020) 083C01.
- [5] M. Gronau and D. London, Phys. Lett. B **253**, 483 (1991); M. Gronau and D. Wyler, Journal Phys. Lett. B **265**, 172 (1991).
- [6] M. Gronau, Phys. Lett. B **557** (2003) 198, arXiv:hep-ph/0211282.
- [7] Heavy Flavor Averaging Group, Y. Amhis et al., arXiv:1909.12524 [hep-ex] (2019).
- [8] J. de Favereau et al., Journal of High Energy Physics **2014** (Feb. 2014).
- [9] C. Helsens and the FCC software group, <https://github.com/HEP-FCC/FCCAnalyses>.
- [10] FCC Collaboration, A. Abada et al., The European Physical Journal Special Topics **228** (2019) 261.
- [11] F. Bedeschi, Code available as part of the Delphes package, <https://github.com/delphes/delphes>.
- [12] T. Suehara and T. Tanabe, Nucl. Instrum. Meth. A **808** (2016) 109.
- [13] N. Bacchetta et al., arXiv:1911.12230 (2019).